Nat. Hazards Earth Syst. Sci. Discuss., 2, 963–997, 2014
www.nat-hazards-earth-syst-sci-discuss.net/2/963/2014/
doi:10.5194/nhessd-2-963-2014

Natural Hazards and Earth System Sciences
Discussions
Open Access

A hybrid model for mapping simplified seismic response via a GIS-metamodel approach

G. Grelle, L. Bonito, P. Revellino, L. Guerriero, and F. M. Guadagno

Department of Sciences and Technologies – University of Sannio, Via de Mulini 59/A, 82100 Benevento, Italy

Received: 9 January 2014 – Accepted: 22 January 2014 – Published: 3 February 2014

Correspondence to: G. Grelle (gegrelle@unisannio.it)

Published by Copernicus Publications on behalf of the European Geosciences Union.

Abstract

An hybrid model, consisting of GIS and metamodel (model of model) procedures, was introduced with the aim of estimating the 1-D spatial seismic site response. Inputs and outputs are provided and processed by means of an appropriate GIS model, named GIS Cubic Model (GCM). This discretizes the seismic underground half-space in a pseudo-tridimensional way. GCM consists of a layered parametric structure aimed at resolving a predicted metamodel by means of pixel to pixel vertical computing. The metamodel leading to the determination of a bilinear-polynomial function is able to design the classic shape of the spectral acceleration response in relation to the main physical parameters that characterize the spectrum itself. The main physical parameters consist of (i) the average shear wave velocity of the shallow layer, (ii) the fundamental period and, (iii) the period where the spatial spectral response is required. The metamodel is calibrated on theoretical spectral accelerations regarding the local likely Vs-profiles, which are obtained using the Monte Carlo simulation technique on the basis of the GCM information. Therefore, via the GCM structure and the metamodel, the hybrid model provides maps of normalized acceleration response spectra. The hybrid model was applied and tested on the built-up area of the San Giorgio del Sannio village, located in a high-risk seismic zone of Southern Italy.

1 Introduction

In earthquake-prone areas, microzonation studies assume a main role in urban planning and managing seismic risk. For this purpose, several studies have been proposed by several authors with the aim of consolidating knowledge on local amplification (e.g. Grasso and Maugeri, 2012; Bianchi Fasani et al., 2008; Scott et al., 2006; Thuladar et al., 2004; Maresca et al., 2003) or introducing methods and procedures aimed at evaluating or estimating the seismic site response (e.g. Papadimitriou et al., 2008; Kienzle et al., 2006; Jimenez et al., 2000). Microzonation studies are developed at three different detail levels and depths (ISSMGE-TC4, 1999), depending on the type and amount of geological, geotechnical and geophysical data available. Conversely from the first two levels, the third level of detail analytically quantifies the seismic response by providing building design parameters. Many building codes, like Eurocode 8 and FEMA 356, usually require seismic design actions to be mainly expressed in terms of spectral acceleration corresponding to the amplified ground motion with respect to expected seismic frequency in bedrock shaking.

In addition to a need to have a sufficient amount of information suitable for the seismic microzonation approached, computerized data management and spatial distribution in terms of both input and output/outcome is also a requirement. Therefore, Geographic Information Systems (GIS) contribute the most to maximizing the available data in assessing or estimating ground-motion amplification (Kolat et al., 2006; Ganapathy, 2011; Hashemi and Alesheikh, 2012; Turk et al., 2012; Hassanzadeh et al., 2013) as well as seismo-induced effects (Grelle et al., 2011; Grelle and Guadagno, 2012). To this regard, literature suggests approaches based on experimental geophysical methods, such as linear dynamic low-strain measures, firstly from ambient noise, or numerical methods of simulation regarding a non-linear stress strain response during shear wave propagation in the layered cover. In such experimental methods, GIS are largely used in the spatial distribution of predominant site periods and related amplification factors (Al Yuncha and Luzon, 2000). These microzonation methods are more expeditious due to the possibility to use a large amount of low cost data (Mukhopadhyaya and Bormann, 2004). However, methods mainly based on microtremor records and on surface wave analysis provide good results in geological settings characterised by high impedance contrasts (Bonnefoy-Claudet et al., 2009), in addition to not considering the non-linearity effects of the dynamic stress–strain behaviour.

In microzonation studies carried out using numerical methods for estimating and evaluating the seismic site response, GIS provide the spatial distribution of parameters that characterized the seismic motion. Kienzle et al. (2006) approached the microzonation of Bucharest by creating a multi-layer geological model and interpolating the values

NHESSD
2, 963–997, 2014

obtained from the transfer function analysis, in map node points, by using linear modelling software such as Proshake (EduPro Civil System, 1999). In the microzonation of Barcellona (Jimenez et al., 2000), the seismic risk hazard was assessed by using the SERGISAI methodology. In this case, the site response analysis was performed using the 1-D linear equivalent method of SHAKE91 (Idriss and Sun, 1992), which assumes a system of homogeneous, horizontally layered viscoelastic soil deposits.

Recently, automated procedures for calculating seismic soil response have been introduced. In these procedures the calculation of multivariate regression functions is modelled on the response outputs of 1-D non-linear analysis collected in the regional Hellenic dataset (HelGeoRDaS) for different layer soil sequences and input motions (Papadimitriou et al., 2008).

In the light of the above mentioned numerical methods, this study presents a hybrid model that is capable of predicting the spatial simplified seismic response by coupling GIS and metamodel procedures.

The hybrid model is based on a GIS model with a layered structure mainly performing a vertical pixel to pixel calculation using and producing data for and from associated "external-GIS" processes. Among the external GIS processes, the metamodeling (modelling of model) assumes the main role. Metamodeling consists of procedures capable of defining non-physical or quasi-physical trained simple models (data driven models), which aim at emulating the performance of more complex physically based models. Hence, estimate and prediction metamodels permit extending the analysis to a greater number of cases (Doebling et al., 2002). Therefore, the success of these methods on the simplified description of natural phenomena depend both on the regression accuracy and robustness of the regression model (Sen and Akyol, 2010) and on the choice of suitable physical models in the training.

The proposed approach provides spatial distributions of the spectral acceleration response or spectral amplitude response following the seismic-lithological setting, which is generally modelled on all the quantitative and qualitative (regional knowledge) datasets on the seismic subsurface. This approach permits minimizing the well-known errors and limitations linked to the use of the spatial interpolation method when it is applied to highly irregular spatial data such as seismic response parameters. In addition, the hybrid model is based on a GIS-metamodel calibrated on a geophysical and geotechnical local database. This last aspect gives the model the opportunity to be re-calibrated when the dataset is upgraded.

The hybrid model was applied to the built-up area of San Giorgio del Sannio village in Southern Italy, where a large amount of geological, geotechnical and geophysical data was available.

2 Hybrid model

The hybrid model architecture is characterized by clusters of procedures and sub-models (Fig. 1) in which data flow and information are driven in a semi-automated way using a tool-code written in Python 2.7 (van Rossum and Drake, 2001). The code is currently being improved with regards to greater automation and user-friendliness. The main clusters and sub-models of the hybrid model are: (i) the GIS Cubic Model (GCM) introduced in this study, (ii) a metamodeling process, and (iii) pre-processing procedures of inputs on numerical and cartographical datasets. Stemming from this dataset, the data/information flow occurs in sequence cascades between the various clusters, with the exception of a final loop between the GCM and the metamodeling process.

2.1 GIS Cubic Model (GCM)

GCM is a simplified and parameterized geometric model of underground half-space. In this way, GCM is a pseudo-3-D physically-layered model based on feature sets and raster-grid calculations. In the first step, it executes a sequential calculation of raw and pre-treated input data. Subsequently, in the second step, it performs the calculation of data from metamodeling processes driven by instructions from the first step.

The GIS Cubic Model is based on two main elements: layer and zone (Fig. 2). The layer corresponds to a lithological unit with specific dynamic proprieties. The lithological unit, hereafter called “litho-dynamic unit”, is mainly defined in terms of shear wave velocity depth-depending curve, and secondarily by its non-linear dynamic behaviour. The depth depending curves result from the regression analysis of Vs-depth values, which are obtained both from depth and surface seismic geophysical surveys as well as deriving from penetration test parameters or other Vs-correlated parameters from field tests. The layer is fully extended but it identifies the corresponding litho-dynamic unit only where this latter is present. The zone is identified by the vertical combination of litho-dynamic units in relation to their presence/absence in the layer sequence.

The model is set on a “matrix structure” having a dimension $n \times m$, where n is the number of i-layers constituting the fields of the polygon features, and m is the number of j-zones forming the records of the polygon features.

The GCM claims that the number of layers is generally equal to the number of litho-dynamic units, but it may be greater when one or more litho-dynamic units are repeated in the sequence. The layer position in the sequence is usually in accordance with the chronostratigraphic relationship. In the matrix structure of n-layer sequence, a layer is defined as empty, assuming a value of 0, when the corresponding litho-dynamic unit is not present. Diversely, it assumes a value of 1 if the layer is filled (Fig. 2). Therefore, given an n-layer sequence, the maximum possible number of m-zones is 2^{n-1}. The bedrock is the nth layer at the base of the sequence, and it is always present in a matrix structure assuming a value of 1. A complete sequence shows all litho-dynamic units present in a study area. Two or more types of bedrock involve the multiplication of maximum possible zones in relation to the number of bedrocks.

2.2 Preliminary analysis and identification of layers and zones

The recognition and delimitation of the zones is a key point due to the fact that they entail the distribution of a one-dimensional layered model, and therefore the associated seismic response.

NHESSD
2, 963–997, 2014

The geometrical delimitation of zones requires qualitative and quantitative data. A preliminary delimitation based on surface geology can be obtained from field surveys and pre-existing maps. The presence and therefore the spatial extension of litho-dynamic units in the layers is defined by understanding the combined data obtained from borehole drilling and surface geophysical surveys. The spatial distribution of the thickness of the layers, is carried out by means of the map interpolation technique for the definition of the zones. Such a distribution is obtained by the identification of the litho-dynamic units and the interpretation of the litho-stratigraphic profiles in accordance with available seismic-logs. In a preliminary phase, the space-identification of the litho-dynamic unit in the layer is associated to an assigned minimum layer thickness. Therefore, taking into account this aspect, layers that in seismic-logs show a thickness less than the minimum layer thickness are considered empty and the thickness must be associated to the next litho-dynamic units. Consequently, the zones have litho-dynamic sequences with a thickness not less than the minimum layer thickness. In the preliminary step, the unconfined interpolation of thickness can be performed for all the layers. In a second subsequent step, the values of layer thickness less than the minimum layer thickness are re-assigned to zero, identifying the non space-presence of the lithodynamic unit present. In addition, the minimum layer thickness value corresponds to the depth at which the seismic response output is defined. This depth is usually associated to the mean foundation plane of a building.

2.3 Shear waves velocity depth-dependent curves

The model requires that the shear wave velocities associated to the cover layer are non linear depth-dependent according to a space-invariant function. Rigid bedrock assumes a constant velocity value. If the bedrock is not rigid, the model expects that the rigid condition is reached by a linear depth-dependent function. Therefore, the function is a non-linear-log for coverage layers:

$$\mathrm{Vs}_i(z) = \mathrm{Vs}_{0_i} + \alpha_i \log(1+z) \qquad (1)$$

NHESSD
2, 963–997, 2014

and for bedrocks:

$Vs_n(z) = Vs_{0_n} + \alpha_n z$ (when non-rigid);

with the condition that $\alpha_n = 0$ (when rigid); (2)

where z is the depth, Vs_0 and α, are the intercept and the gradient, respectively, obtained via the regression analysis of Vs-depth data.

In predictive terms, the empirical shear wave velocity curves given by Eqs. (1) and (2) are the best representative values taking into account an increase of the stiffness due to the lithostatic load (Fig. 3). In agreement with the matrix structure of the GCM, the shape of the bedrock and cover layers functions takes into consideration the same number of coefficients. The linear-log function assumed for the cover layer seems to have a fit-performance close to the three-parameter power function usually used in regression Vs depth-dependent analysis (Robertson et al., 1995).

In non-rigid bedrock, the linear function establishes that the shear-wave velocity increases downward with the depth until this velocity assumes the value assigned to the rigid bedrock (e.g. $800\,\mathrm{m\,s^{-1}}$) (Fig. 3). In addition, there is the need for the intercept velocity of the non-rigid bedrock function to be greater than/or equal to the function of the cover litho-dynamic units. This aspect reflects a condition, and assumption, where non-rigid bedrocks must be more rigid than litho-dynamic cover units and, therefore, they reach a rigid condition much quicker at a depth than these latter.

2.4 First stage procedure in GCM

A new matrix named "parameters matrix" with dimensions of $2n \times m$ was added to the structure matrix. In both matrices, zero values are corresponding. Values introduced in the parameters matrix are real coefficients stemming from depth–Vs regression analysis. The structure matrix fields and the parameters matrix fields were converted to raster and distributed over the whole area. The raster parameters are layer$_i$, V_{0_i}, α_i and $h_{i(x,y)}$, and their processes (progressions) are the following raster mathematical operations:

NHESSD
2, 963–997, 2014

(i) the spatial limitation of the thickness of the layers, and consequently of the zones, is obtained through a raster-calculation cutting: $h_{i(x,y)} = h^*_{i(x,y)} \cdot \text{layer}_i$, where $h^*_{i(x,y)}$ is the ith layer thickness raster obtained by usual spatial interpolation methods under an unconfined condition. The raster cutting sets to zero the possible interpolated residual thickness in zones where the litho-dynamic unit is not present.

(ii) The shear-wave velocity at the top and bottom of each n-1 cover layer is obtained using the parameterized log-linear functions.
The vertical shear-wave velocity distribution of the cover layers can also admit inversion rigidity conditions in relation to their position (Fig. 3).

$$\mathrm{Vs}^{\mathrm{TOP}}_{i(x,y)} = \mathrm{Vs}_{0_i} + \alpha_i \left\{ \ln \left[1 + \left(\sum_{i=1}^{n-1} h_{i-1(x,y)} \right) \right] \right\} \tag{3}$$

$$\mathrm{Vs}^{\mathrm{BOT}}_{i(x,y)} = \mathrm{Vs}_{0_i} + \alpha_i \left\{ \ln \left[1 + \left(\sum_{i=1}^{n-1} h_{i(x,y)} \right) \right] \right\} \tag{4}$$

(iii) With regard to rigid bedrock (nth layer), it is defined by a unique value of shear-wave velocity.
When the bedrock is non-rigid (geological bedrock), it is possible to assign a thickness of $h_{n(x,y)}$ down to the rigid condition; in relation, the model necessitates the assignment of a shear waves velocity to the rigid bedrock, e.g. bedrock velocity $\mathrm{Vs}^{\mathrm{BOT}}_{n(x,y)} = 800\,\mathrm{m\,s^{-1}}$ (EC8 prEN1998). This parameter is therefore defined by the following equation:

$$h_{n(x,y)} = \left(800 - \mathrm{Vs}^{\mathrm{TOP}}_{n(x,y)}\right)/\alpha_n; \quad \text{where } \mathrm{Vs}^{\mathrm{TOP}}_{n(x,y)} = \max\left(\mathrm{Vs}^{\mathrm{BOT}}_{n-i(x,y)}, \mathrm{Vs}_{0_n}\right) \tag{5}$$

where α_n is the gradient and the $\mathrm{Vs}^{\mathrm{TOP}}_{n(x,y)}$ is equal to max values between $\mathrm{Vs}^{\mathrm{BOT}}_{n-i(x,y)}$,the shear wave velocity of the end cover litho-dynamic unit and the Vs_{0_n},

NHESSD
2, 963–997, 2014

the intercept value of the bedrock Vs-depth regression curve. De facto, Eq. (5) takes into account the possible head rigidity increase due to lithostatic layer cover loads in non rigid bedrock (relatively low Vs values) or this increase is not contemplated in the presence of quasi rigid bedrock (relatively high Vs values).

(iv) The spatial distribution of shear-wave velocity at the top and bottom of the layers allows for defining the raster of the average shear-wave velocity of each litho-dynamic unit:

$$\overline{\mathrm{Vs}}_{i(x,y)} = \frac{1}{2}\left(\mathrm{Vs}^{\mathrm{TOP}}_{i(x,y)} + \mathrm{Vs}^{\mathrm{BOT}}_{i(x,y)}\right) \quad (6)$$

(v) The average shear-wave velocity defines the raster of the fundamental vibration period:

$$T_{0(x,y)} = \frac{4\sum_{i=1}^{n} h_{i(x,y)}}{\sum_{i=1}^{n}\left(\overline{\mathrm{Vs}}_{i(x,y)} h_{i(x,y)}\right) / \sum_{i=1}^{n} h_{i(x,y)}} \quad (7)$$

2.5 Metamodeling processes

The metamodeling process aims at obtaining prediction models generated and trained on an output dataset resulting from a seismic site response analysis performed on the simulation of layered Vs-profiles. In this way, the obtained model is used to predict the seismic response of similar layering Vs-profiles in a simplified manner.

– *Generation of vertical layering Vs-profiles*

The generation of the layered Vs-profiles is performed by means of the Monte Carlo simulation technique of $n-1$ cover layers. This simulation technique is based on an uniform random distribution. It is suitable in a linear gradient and a multimodal distribution of the thickness of the layers. Alternatively, other simulation techniques based on the Gaussian distribution can be used for this purpose. The choice of the thickness of the layers occurs within the assigned interval in which the maximum and minimum values are defined by the GCM. The thickness of the *n*th layer is zero in the case of rigid bedrock. Instead, when the bedrock is non-rigid, its thickness is the function of the depth reached by the cover layer sequence (Eq. 5) once the shear-wave velocities of the cover bottom sequence are defined (Eq. 4). For a better prediction performance of the model, the number of profiles generated must take into account the width of the thickness of the existing interval and the number of layers that characterize each zone.

– *1-D seismic response*

On the simulated layered Vs-profiles that are representative of each zone, the seismic response is defined by numerical methods that compute the seismic wave propagation in the subsoil (e.g. EERA, SHAKE, NERA etc.). These methods are based on the 1-D shear wave propagation from the rigid bedrock within a plane-parallel layered subsoil. In terms of total stress, the dynamic behaviour is analyzed using a viscoelastic constitutive shear stress–strain relation. However other numerical models can be used. The calculation requires the basic seismic input and the layered Vs-profiles which are parameterized in terms of shear waves velocity, Vs, density, ρs the reduction curve of shear normalized modulus, G/G_0, and damping curves, D/D_0.

In order to increase analysis accuracy, the layered Vs-profile can be further divided into sub-layers having the corresponding shear velocity computed by Eqs. (1) and (2). The result is the damped-elastic acceleration response spectra, SA, and it stems from the fixed depth within the shallow layers (mean foundation plane). Successively, the normalized acceleration response spectra, NSA, is obtained in relation to the response spectrum which refers to the outcrop bedrock.

Discrete NSA_T values are sampled/selected in a spectral window where the amplification is significantly high for all the 1-D-models representing the zones.

– *Data driven modelling*

The sampled/selected NSA values constitute the training and validation dataset used in the multivariate regression analysis. The dataset consists of eighty-two spectral series of six cover zones and two non-rigid bedrock zones, in which eight NSA_T values were selected, for a total of 648 training theoretical parameters. This dataset refers to the application case of the hybrid model outlined below.

Eureqa Formulize (Schmidt and Lipson, 2009, 2013), which creates evolutionary equations using genetic programming, was used to develop the prediction model. This model is sustained by a sensitivity analysis in order to define the Principal Component Regression (PCR). The Principal Components are: (i) the simulated average shear-wave velocities of the shallow layers, $\overline{\mathrm{Vs}}^{\mathrm{UP}}$, (ii) the simulated elastic fundamental period T_0 and (iii) the identified periods, T. The first two are the endogenous variables directly related to the performance of the regression modelling, due to the fact that they are linked to the physical nature of the phenomena. In contrast, the spectral period T is the exogenous variable introduced to identify the spectral position of the predicted NSA_T values.

Using the aforementioned variables, and by means of semi-automatic modelling, an effective and efficient regression model constituted by a bilinear-polynomial equation was developed. The equation of the prediction model in generic x, y map points is:

$$\mathrm{NSA}_{T(x,y)} = a_1 \overline{\mathrm{Vs}}^{\mathrm{UP}}_{(x,y)} + a_2 T + \sum_{k=1}^{4} b_k (T_{0(x,y)} - T)^k \tag{8}$$

where a_1 and a_2 are linear coefficients while b_k are the polynomial coefficients. For each 1-D layered model, the calibrated coefficients can be calculated by iterative methods, for example the least squares methods, in order to minimize error.

In reference to the physical nature of spectral curves, the variables assumed in the polynomial of Eq. (8) promote a best fitting performance. This variable is in relation to fundamental period and it favours a flexible fitting of spectral shapes in large or small peak cases. However, in order to ensure a greater performance in the calibration phase, the theoretical spectral values must be selected in the window where the spectral amplification is substantial.

2.6 Second stage procedure in GCM

The second stage of the GCM allows the $NSA_{T(x,y)}$ spatial distribution to solve the regression equation (Eq. 8), having defined the best calibration coefficients. The fundamental period $T_{0(x,y)}$ is calculated in the first step (Eq. 7).

The spatial distribution of the simplified models from a regression analysis is characterized by an intrinsic jump effect along the border between two zones due to the different performance of the respective prediction models.

This effect is solved by means of an under sampling via a dense regular mesh. Therefore a subsequent redistribution of the $NSA_{T(x,y)}$ values is obtained using a selected spatial interpolation technique.

3 Application and results

The hybrid model was applied in the built-up area of the San Giorgio del Sannio village in the Campania region – Southern Italy. The area has a plain-hill morphology with a surface of 4.8 km^2, a population density of 1500 people per square kilometres, and it is classified as being at high-level seismic-hazard by the official Italian seismic hazard map (NTC, 2008). In addition, the location is close to active tectonic structures which have produced powerful earthquakes in the last two-thousand years (Galatini et al., 2000).

NHESSD
2, 963–997, 2014

3.1 Lithological and geophysical features

Pre-existing geological studies and field investigations highlight that the bedrock consists of Pliocene-marine deposits, while the cover layers are Quaternary terrains deposited in a fluvio-lacustrine environment and more recent pyroclastic deposits. Together with the above qualitative data, depth investigations permitted the identification of lithological units that also took into account the rigidity of material. A total of 177 boreholes, with a depth from ten to forty meters, 15 multichannel analyses of surface waves (MASW), 4 down holes, and 2 H/V spectral ratios from ambient noise records permitted an investigation of the cover layers and thus an identification of the following related litho-dynamic units (Fig. 4):

(i) layer 1 – PIR, air-fall and/or flow pyroclastic deposits. The particle-size distribution characterises them as being mono-granular sands. Thin layers of pumices of gravel size are frequently present;

(ii) layer 2 – FLR, recent fluvio-lacustrine deposits consisting of loose sands;

(iii) layer 3 – FLA, ancient fluvio-lacustrine deposits consisting of smaller, thickened gravelly-sand, sand and silty-sand.

The bedrock is faulted. The dislocation placed it in contact with two deposits that have approximately the same age:

(iv) layer 4a – SBC, thickened, stratified granular deposits, mainly sandy conglomerates;

(v) layer 4b – GRL, stiff blue clay/silt.

Both units show characteristics of a non-rigid bedrock.

NHESSD
2, 963–997, 2014

3.2 Model application and calibration

The identified layered-sequences determine the eight zones. Zone 1 and 2 are two bedrock layers, while the combinations of the cover layers define six zones from 3 to 8, where the latter shows the litho-dynamic complete sequence (Fig. 4).

Based on the litho-dynamic units detected, the distribution of the thickness of the layers was determined by means of a "topo-to-raster" interpolation technique (Hutchinson, 1996) using the data points that defined the stratigraphic-log and geophysical surveys.

With regards to the cover layers, the depth-distribution of the shear-wave velocities (Fig. 5) show low values for pyroclastic soils and recent fluvio-lacustrine deposits. In contrast, larger values are displayed in ancient fluvio-lacustrine deposits. A large amount of surveys exist for ancient fluvio-lacustrine deposits, due to the fact that these deposits are widely present in the whole area.

The depth-distributions of shear-wave velocities within the bedrock layers have shown their non-rigid nature at shallow depths. Thickened granular stratified deposits, SBC, have shown a greater increase of depth-dependent shear-wave velocities in relation to stiff blue clay/silt, GRL. Shear-wave velocity values at the bedrock are frequently detected in the undercover condition. However, in the linear regression analysis, an intercept value is imposed equal to the ancient fluvio-lacustrine deposits as foreseen by the model (Sect. 2.3).

Once completed, the structural and parametric matrix gives the possibility to define the average shear-wave velocities and thickness of the layers in accordance with the elastic fundamental period mapped in the GIS Cubic Model (Fig. 6).

The thickness distribution of the layers permits defining the limit values of the possible layered profiles characterizing the eight detected zones. On the basis of these values, the simulated-layered Vs-profiles were generated using the Monte Carlo technique (Fig. 7). In this way, the number of profiles is assumed taking into account the number and extension of the layers constituting the zone. Ten to fifteen profiles were generated on these zones in which the cover layers were present. Subsequently, an additional half-division function of depth was performed for the simulate profile including the cover layer (zones from 3 to 8), while a multi-division was performed for the profiles simulating the outcropping bedrock (zones 1 and 2) (Fig. 7).

Using the simulate Vs-profile, the numerical analysis of the seismic response was performed by means of the NERA code, Non-linear Earthquake site Response Analysis (Bardet and Tobita, 2001). The code permits resolving the seismic motion equation in the time domain taking into consideration the vertical propagation of the shear waves in a layered medium having a non-linear hysteretic stress–strain behaviour. The constitutive IM-model implemented in NERA was proposed by Iwan (1967) and Mroz (1967). This model foresees that the shear-stress–strain hysteretic loop follows the Masing's model. The damping curves ratio are derived from normalized rigid module curves G/G_0 that cannot be introduced into the independent modality in contrast to the linear equivalent models. Usually the experimental damping curves are used for a comparison with theoretical curves.

The input motion used in the response analysis was defined in accordance with regional seismic hazard studies as reported in technical regulations for constructions (NTC 2008). The input motion is spectrum-compatible with the elastic horizontal spectral response acceleration corresponding to 10 % exceedance probability over a 50 yr time interval; this spectrum refers to the life preservation state in normally crowded buildings. Disaggregation analysis, performed by Rexel 3.5 beta computer software (Iervolino et al., 2009), shows that the major hazard spectral contribution refers to earthquakes with a local magnitude between 6.5 and 7.0 and a distance between 15 and 20 km. Taking into account the afore-mentioned studies, the seismic input was obtained from the north-southern real-time-history component of the Irpinia earthquake (year 1980 with 6.9 M_w) recorded by the Bagnoli Irpino strong-motion station, located 20 km from the study area, with a epicentral distance of 30 km at the earthquake time.

Normalized shear modulus reduction and damping ratio curves were obtained from the literature regarding this subject (Guadagno et al., 1998; Zhang et al., 2005), taking into account lithology, granular size distribution and Vs or SPT (Fig. 8).

The output acceleration response spectra is defined at 5 % of damping and it refers to a depth of three meters from the ground surface. Eight NSA_T values were extracted from a sampling of 0.10 s within the period-window 0.00 s (PGA)–0.70 s; in this range, most of the amplifications were shown for all layered models (zones).

Therefore, 648 NSA_T values were obtained for 82 series simulating the eight layered models; these values constitute an equal ratio of training and validation dataset used in the multiple calibration coefficient analysis (Table 1) of the prediction model defined by Eq. (9). Therefore, the best performance of the model (Table 2) in regression analysis was detected in relation to minimum Mean Squared Error.

The second step of the GCM determined the average shear-wave velocity raster of the shallow layers (Fig. 6). Subsequently, the $NSA_{T(x,y)}$ rasters were obtained from Eq. (9) using the calibrated coefficient. Finally, the spatial smoothing of $NSA_{T(x,y)}$ was performed by an under sampling with a 50 m regular mesh (Fig. 9).

4 Validation and discussion

The hybrid model is characterized by a sequence of physical-mathematical processes to produce simplified maps regarding spectral acceleration response values at different identified discrete-periods. The simplification involves many components of the model, each of them influencing different degrees of the estimation/prediction performance of the very same model. This aspect may be attributed to the following features: (i) the coherent identification and subdivision of the litho-dynamic units. The dispersion of the velocity with the depth is associated with such a coherence; (ii) the efficiency of a prediction model for any given 1-D-layered model zone; (iii) the uncertainties and approximations due to the 1-D numerical modelling when it is used in concomitance with a complex-layering setting; (iv) the spatial distribution techniques used.

The performance of prediction/estimation of the hybrid model was validated on four down-hole locations where the stratigraphic-logs and the velocity profiles are experimentally known (Fig. 10). The depth-extension of some Vs-profiles to the rigid bedrock were performed in relation to the spatial distribution of the rigid bedrock depth resulting from the GCM model. Thus, by comparing the spectra acceleration numerical response with the hybrid model $\mathrm{NSA}_{T(x,y)}$ values, a good validation feedback in the spectral amplification window (0.00–0.70 s) is highlighted. An almost similar approximation is shown with and without spatial smoothing output. In addition, the validation test shows that the regression functions obtained by the metamodeling process can be directly used for the local definition of seismic response values in the same spectra periods chosen in the hybrid model. However, the Vs experimental profiles necessitate simplification in accordance with the 1-D-layered model defined for the hybrid model processing. Accuracy must be carried out in the identification of the average shear waves velocity, $\overline{\mathrm{Vs}}^{\mathrm{UP}}_{(x,y)}$, attributed at the shallow layer. This layer must be defined taking into account that it is referred to a litho-dynamic unit (Fig. 10).

The prediction model defined and tested on the eight layered-model-series highlights a good degree of accuracy and precision, showing correlation coefficients, R, ranging between 0.83 and 0.92. This short range, in addition to the low complexity of the regression function [9] confers to the model the requirements of predictive accuracy and robustness. The efficacy of the predictors, $\overline{\mathrm{Vs}}^{\mathrm{UP}}_{(x,y)}$ and T_0, is supported by the fact that they are used in the definition of curves and abacuses regarding the estimate procedure of site amplified factors (Pergalani and Compagnoni, 2008).

Calculation of fitting errors disaggregated spectral analysis (graphic in Fig. 9) shows that the fitting performance of the model is variable with the period and it seems that error in several cases is greater nearer to PGA values and subordinate to the fundamental periods. Such analysis should be carried out and reported in the $\mathrm{NSA}_{T(x,y)}$ maps, aimed at providing accuracy in estimation in relation to expected ground-building structure resonance.

NHESSD
2, 963–997, 2014

5 Conclusions

This paper introduces a hybrid model with the purpose of mapping simplified local seismic response in areas characterized by stratified sequences featured by low geometrical complexity. This method is based on a GIS model, named GIS Cubic Model, and metamodeling processes.

The GCM is a layered model constructed for spatial calculation and distribution of 1-D models composed of litho-dynamic units, known as "layers". The latter are defined by detected and defined lithological units that are characterized by shear-wave depth-dependent curves and consequently by non-linear stress–strain behaviours. The combination of the litho-dynamic sequences constitutes the "zone".

The metamodeling process carries out a regression analysis on data of local seismic responses regarding layered profiles that simulate the possible Vs-profiles observable in a generically-defined zone. In this work, we propose simulated profiles obtained using the Monte Carlo technique.

The prediction model results from a metamodeling process, a bi-linear polynomial mathematical shape in which the exogenous predictors are the shear waves velocity of the shallow layer, $\overline{\mathrm{Vs}}^{\mathrm{UP}}_{(x,y)}$, and the fundamental period, T_0; the period T constitutes the endogenous predictor detecting the spectral coordinates of the normalized spectral acceleration, $\mathrm{NSA}_{T(x,y)}$, within the spectral window where the amplification is shown.

The application and the development of the method was carried out in the urban area of the San Giorgio del Sannio village in Southern Italy. In this area a great number of geognostic and geophysical surveys are present in addition to up-to-date geological maps. All this information permits the use of 1-D numerical modelling of the seismic site response.

In this context, the metamodeling processes created an output data set of eight Vs-layered simulated profiles that were processed through the NERA code. For all the areas, the prediction model proved to be sufficiently robust and accurate.

Moreover, the back-validation test was performed in zones where experimental profiles of 4 down-holes were present. Depending on the case, test results highlighted a high-to-good fit between the values of the spectral response of the hybrid model and those calculated from the physically based numerical model.

Therefore, considering the nature of the mapped quantitative information, the hybrid model aspires to perform a third level of ground motion seismic microzonation.

References

Al Yuncha, Z. and Luzon, F.: On the horizontal-to-vertical spectral ratio in sedimentary basins, B. Seismol. Soc. Am., 90, 1101–1106, 2000.

Bardet, J. P. and Tobita, T.: NERA: A Computer Program for Nonlinear Earthquake site Response Analyses of Layered Soil Deposits, University of Southern California, United States, 2001.

Bianchi Fasani, G., Cavinato, G. P., Petitta, M., Scarascia Mugnozza, G., and Voltaggio, M.: The geological model of Celano town area for seismic microzonation activities, Soil Dyn. Earthq. Eng., 28, 978–985, 2008.

Bonnefoy-Claudet, S., Baize, S., Bonilla, L. F., Berge-Thierry, C., Pasten, C., Campos, J., Volant, P., and Verugo, R.: Site effect evaluation in the basin of Santiago de Chile using ambient noise measurements, Geophys. J. Int., 176, 925–937, 2009.

Doebling, S. W., Hemez, F. M., Schultze, J. F., and Cundy, A. L.: A metamodel-based approach to model validation for nonlinear finite element simulations, 20th International Modal Analysis Conference, Los Angeles, CA, USA, February 2002, 4753, 671–678, 2002.

Galadini, F. and Galli, P.: Active tectonics in the Central Apennines (Italy) – input data for seismic hazard assessment, Nat. Hazards, 22, 225–270, 2000.

Ganapathy, G. P.: First level seismic microzonation map of Chennai city – a GIS approach, Nat. Hazards Earth Syst. Sci., 11, 549–559, doi:10.5194/nhess-11-549-2011, 2011.

Grasso, S. and Maugeri, M.: The seismic microzonation of the City of Catania (Italy) for the Etna Scenario earthquake ($M = 6.2$) of 20 February 1818, Earthq. Spectra, 28, 573–594, 2012.

Grelle, G. and Guadagno, F. M.: Regression analysis for seismic slope instability based on double phase viscoplastic sliding model of the rigid block, Landslides, 10, 583–597, doi:10.1007/s10346-012-0350-8, 2013.
Grelle, G., Revellino, P., and Guadagno, F. M.: Methodology for seismic and post-seismic stability assessing of natural clay slope based on a visco-plastic behavioural model in simplified dynamic analysis, Soil Dyn. Earthq. Eng., 12, 1248–1260, 2011.
Guadagno, F. M., Nunziata, C., and Rapolla, A.: Dynamic parameters of volcaniclastic soils and rocks of Campi Flegrei (Italy), in: Volcanic Seismology, IAVCEI Proceedings in Volcanology, 3, Springer-Verlag, 533–546, 1992.
Hashemi, M. and Alesheikh, A. A.: Development and implementation of a GIS-based tool for spatial modeling of seismic vulnerability of Tehran, Nat. Hazards Earth Syst. Sci., 12, 3659–3670, doi:10.5194/nhess-12-3659-2012, 2012.
Hassanzadeh, R., Nedoviæ-Budiæ, Z., Alavi Razavi, A., Norouzzadeh, M., and Hodhodkian, H.: Interactive approach for GIS-based earthquake scenario development and resource estimation (Karmania hazard model), Comput. Geosci., 51, 324–338, 2013.
Hutchinson, M. F.: A locally adaptive approach to the interpolation of digital elevation models, in: Proceedings, Third International Conference/Workshop on Integrating GIS and Environmental Modeling, Santa Barbara, CA, National Center for Geographic Information and Analysis, available at: http://www.ncgia.ucsb.edu/conf/SANTA_FE_CD-ROM/sf_papers/hutchinson_michael_dem/local.html, 1996.
Idriss, I. M. and Sun, J. I.: "User's Manual for SHAKE91", Center for Geotechnical Modeling, Department of Civil Engineering, University of California, Davis, 1992.
Iervolino, I., Galasso, C., and Cosenza, E.: REXEL: computer aided record selection for code-based seismic structural analysis, B. Earthq. Eng., 8, 339–362, 2009.
ISSMGE-TC4: Manual for zonation on seismic geotechnical hazards, The Japanese Society of Soil Mechanics and Foundation Engineering Multidisciplinary Center for Earthquake Engineering Research, MCEER, 1995, 1999.
Iwan, W. D.: On class of models for the yielding behaviour of continuous and composite systems, J. Appl. Mech., 34, 612–617, 1997.
Jimenez, M. J., Garcia-Fernadez. M., Zonno, G., and Cella, F.: Mapping sol effects in Barcelona, Spain, through an integrated GIS environment, Soil Dyn. Earthq. Eng., 19, 289–301, 2000.

Kienzle, A., Hannich, D., Wirth, W., Ehret, D., Rohn, J., Ciugudean, V., and Czurda, K.: A GIS-based study of earthquake hazard as a tool for the microzonation of Bucharest, Eng. Geol., 87, 13–32, 2006.
Kolat, Ç., Doyuran, V., Ayday, C., and Lütfi Süzen, M.: Preparation of a geotechnical microzonation model using geographical information systems based on multicriteria decision analysis, Eng. Geol., 87, 241–255, 2006.
Maresca, R., Castellano, M., De Matteis, R., Saccorotti, G., and Vaccariello, P.: Local site effects in the town of Benevento (Italy) from noise measurements, Pure Appl. Geophys., 160, 1745–1764, 2003.
Mróz, Z.: On the description of anisotropic workhardening, J. Mech. Phys. Solids, 15, 163–175, 1967.
Mukhopadhyay, S. and Bormann, P.: Low cost seismic microzonation using microtremor data: an example from Delhi, India, J. Asian Earth Sci., 24, 271–280, 2004.
Papadimitriou, A. G., Antoniou, A. A., Bouckovalas, G. D., and Marinos, P. G.: Methodology for automated GIS-aided seismic microzonation studies, Comput. Geotech., 35, 505–523, 2008.
Pergalani, F. and Compagnoni, M.: A procedure for the evaluation of seismic local effects in Lombardia (Italy) for urban planning, The 14th World Conference on Earthquake Engineering, 12–17 October 2008, Beijing, China, 2008.
Robertson, P. K., Sasitharan, S., Cunning, J. C., and Sego, D. C.: Shear-wave velocity to evaluate in-situ state of Ottawa sand, J. Geotech. Eng.-ASCE, 121, 262–303, 1995.
Schmidt, M. and Lipson, H.: Distilling free-form natural laws from experimental data, Science, 324, 81–85, 2009.
Schmidt, M. and Lipson, H.: Eureqa (Version 0.98 beta) [Software], available at: http://www.eureqa.com/, 2013.
Scott, J. B., Rasmussen, T., Luke, B., Taylor, W. J., Wagoner, J. L., Smith, S. B., and Louie, J. N.: Shallow shear velocity and seismic microzonation of the urban Las Vegas, Nevada, Basin, B. Seismol. Soc. Am., 96, 1068–1077, 2006.
Sen, G. and Akyol, E.: A genetic-algorithm approach for assessing the liquefaction potential of sandy soils, Nat. Hazards Earth Syst. Sci., 10, 685–698, doi:10.5194/nhess-10-685-2010, 2010.
Tuladhar, R., Yamazaki, F., Warnitchai, P., and Saita, J.: Seismic microzonation of the greater Bangkok area using microtremor observations, Earthq. Eng. Struct. D., 33, 211–225, 2004.

Turk, T., Gümüşay, U., and Tatar, O.: Creating infrastructure for seismic microzonation by Geographical Information Systems (GIS): a case study in the North Anatolian Fault Zone (NAFZ), Comput. Geosci., 43, 167–176, 2012.
van Rossum, G. and Drake, F. L.: Python Reference Manual, PythonLabs, Virginia, USA, available at: http://www.python.org, 2005.
Zhang, J., Andrus, R. D., and Juang, C. H.: Normalized shear modulus and material damping ratio relationships, J. Geotech. Geoenviron., 131, 453–464, 2001.

NHESSD
2, 963–997, 2014

A hybrid model for Gis-seismic response

G. Grelle et al.

Table 1. Best calibration coefficients of the metamodel.

Predictor Coefficients	Zone 1 and 2	Zone 3	Zone 4	Zone 5	Zone 6	Zone 7	Zone 8
a_1	2.22×10^{-3}	8.17×10^{-3}	4.56×10^{-3}	5.36×10^{-3}	7.71×10^{-3}	8.29×10^{-3}	8.74×10^{-3}
a_2	1.761	1.135	0.209	−0.520	1.509	1.266	1.769
b_1	1.341	1.737	1.809	0.079	1.593	1.588	2.648
b_2	−3.981	−10.39	−1.652	−4.28	−7.507	−5.115	−6.953
b_3	6.587	−1.757	−10.11	−7.086	1.098	−3.040	−0.177
b_4	29.08	39.732	0.795	1.756	30.663	9.78	30.154

NHESSD
2, 963–997, 2014

A hybrid model for Gis-seismic response

G. Grelle et al.

Table 2. Best performance parameters in regression coefficient analysis.

Best performance	Zone 1 and 2	Zone 3	Zone 4	Zone 5	Zone 6	Zone 7	Zone 8	Mean
Correlation coefficient, R	0.871	0.832	0.853	0.853	0.863	0.922	0.925	–
Maximum Error	0.204	0.444	0.497	0.314	0.332	0.303	0.367	0.352
Mean Squared Error	0.005	0.036	0.016	0.011	0.018	0.011	0.012	0.016
Mean Absolute Error	0.053	0.157	0.097	0.082	0.102	0.084	0.082	0.094

NHESSD
2, 963–997, 2014

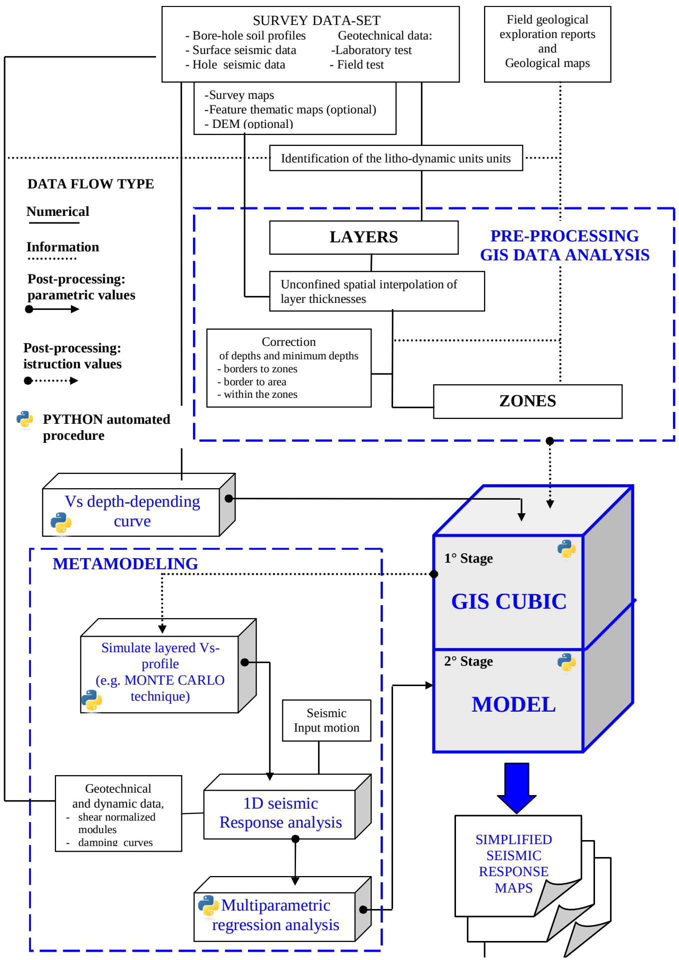

Fig. 1. Flow diagram of hybrid model architecture.

NHESSD
2, 963–997, 2014

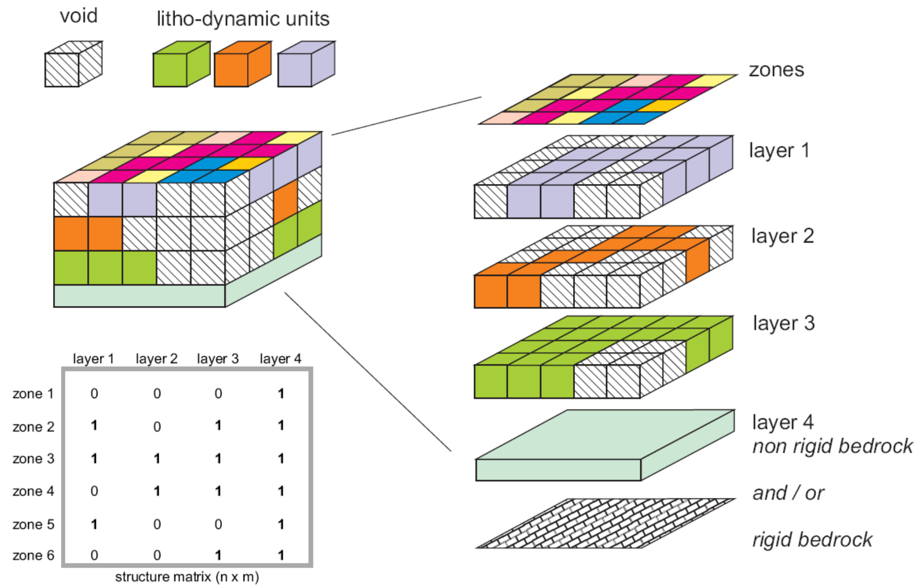

Fig. 2. Subsoil half-space modeling by the GIS Cubic Model and structure matrix, an example using four layers.

NHESSD
2, 963–997, 2014

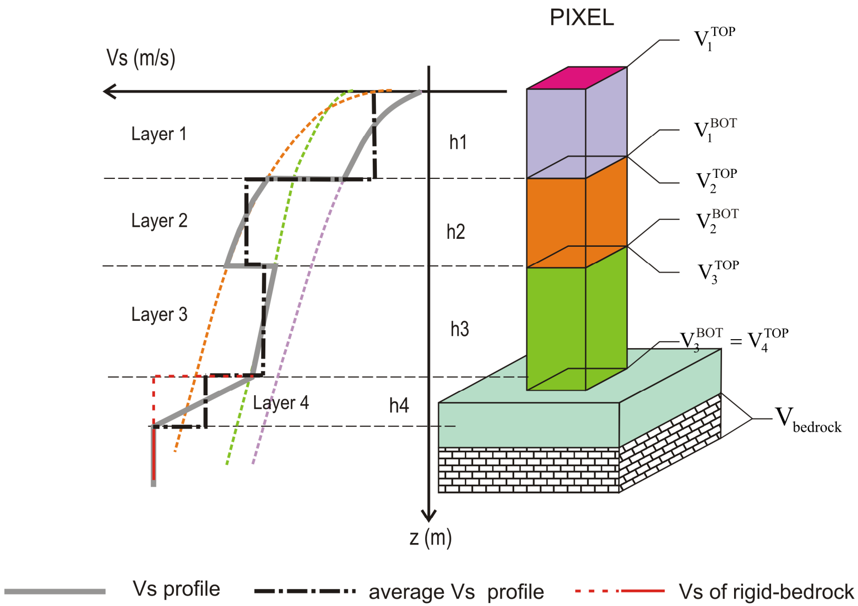

	layer 1	layer 2	layer 3	layer 4	$V_0$1	$V_0$2	$V_0$3	$V_0$4	α1	α2	α3	α4
zone 1	0	0	0	**1**	0	0	0	**<value>**	0	0	0	**<value>**
zone 2	**1**	0	**1**	**1**	**<value>**	0	**<value>**	**<value>**	**<value>**	0	**<value>**	**<value>**
zone 3	**1**	**1**	**1**	**1**	**<value>**	**<value>**	**<value>**	**<value>**	**<value>**	**<value>**	**<value>**	**<value>**
zone 4	0	**1**	**1**	**1**	0	**<value>**	**<value>**	**<value>**	0	**<value>**	**<value>**	**<value>**
zone 5	**1**	0	0	**1**	**<value>**	0	0	**<value>**	**<value>**	0	0	**<value>**
zone 6	0	0	**1**	**1**	0	0	**<value>**	**<value>**	0	0	**<value>**	**<value>**

structure matrix (n x m) parameter matrix (2n x m)

Fig. 3. 1-D layered Vs-profile and parameters matrix GIS Cubic Model, an example using four layers.

NHESSD
2, 963–997, 2014
A hybrid model for Gis-seismic response
G. Grelle et al.

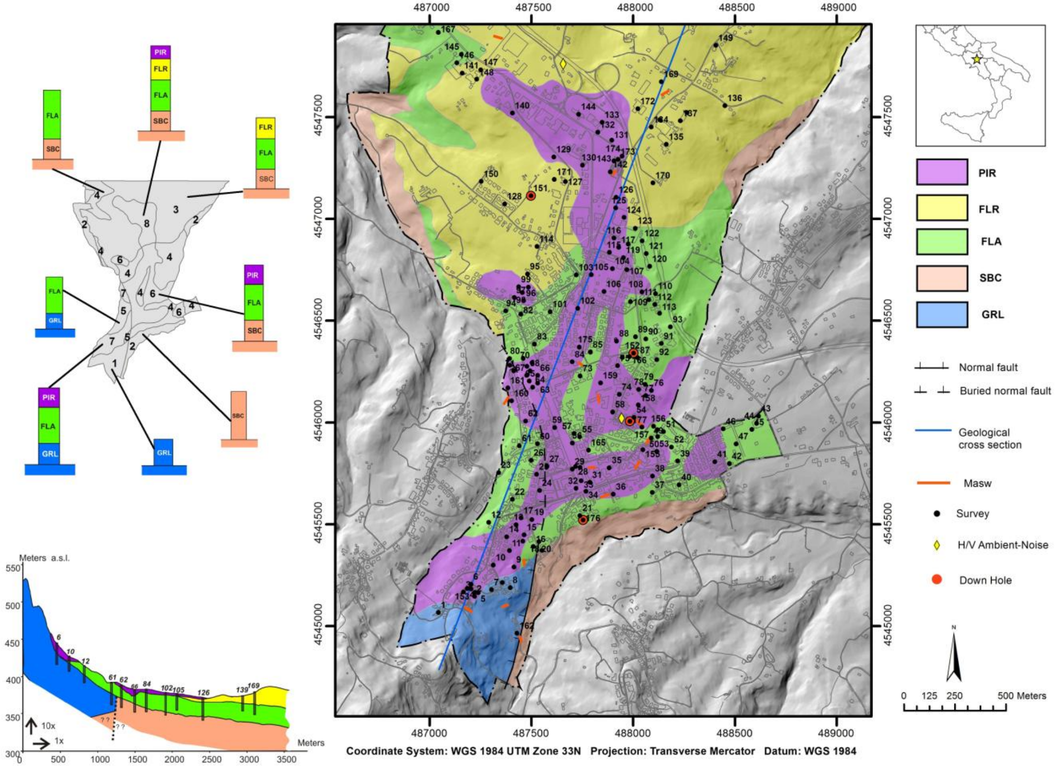

Fig. 4. Litho-dynamic units map, cross-section and zones deriving from 1-D layers combination.

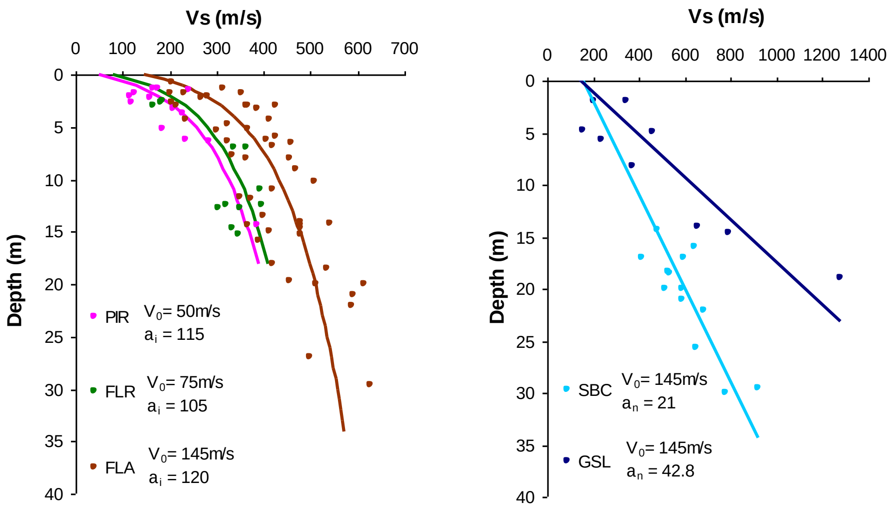

Fig. 5. Vs depth-dependent curves of the litho-dynamic units.

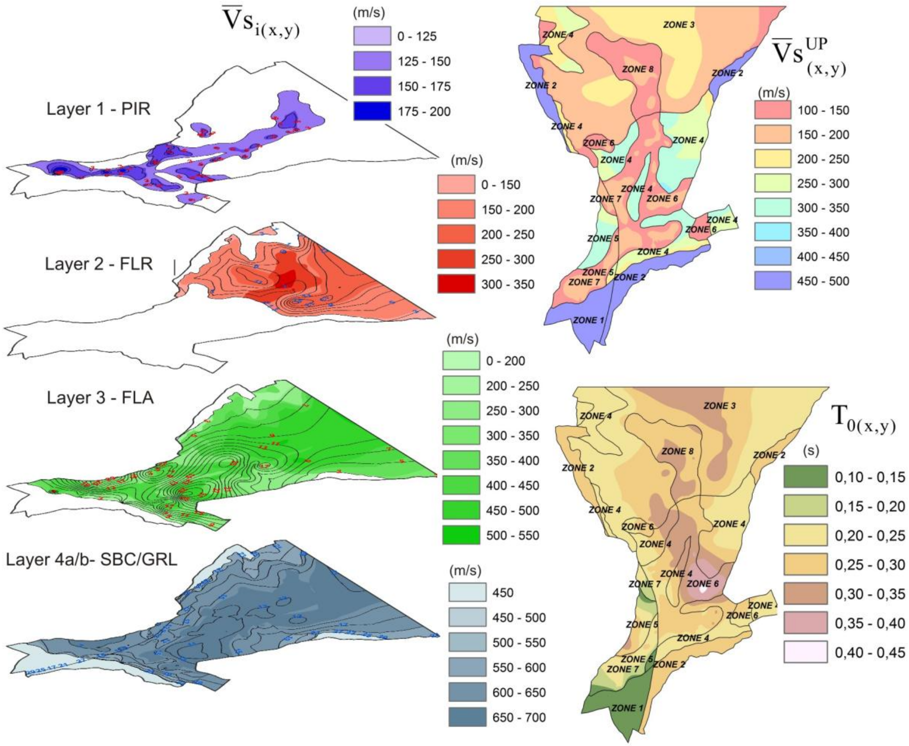

Fig. 6. Maps resulting from the GIS Cubic Model; the average Vs-layering maps report the respective iso-thickness curves.

NHESSD
2, 963–997, 2014

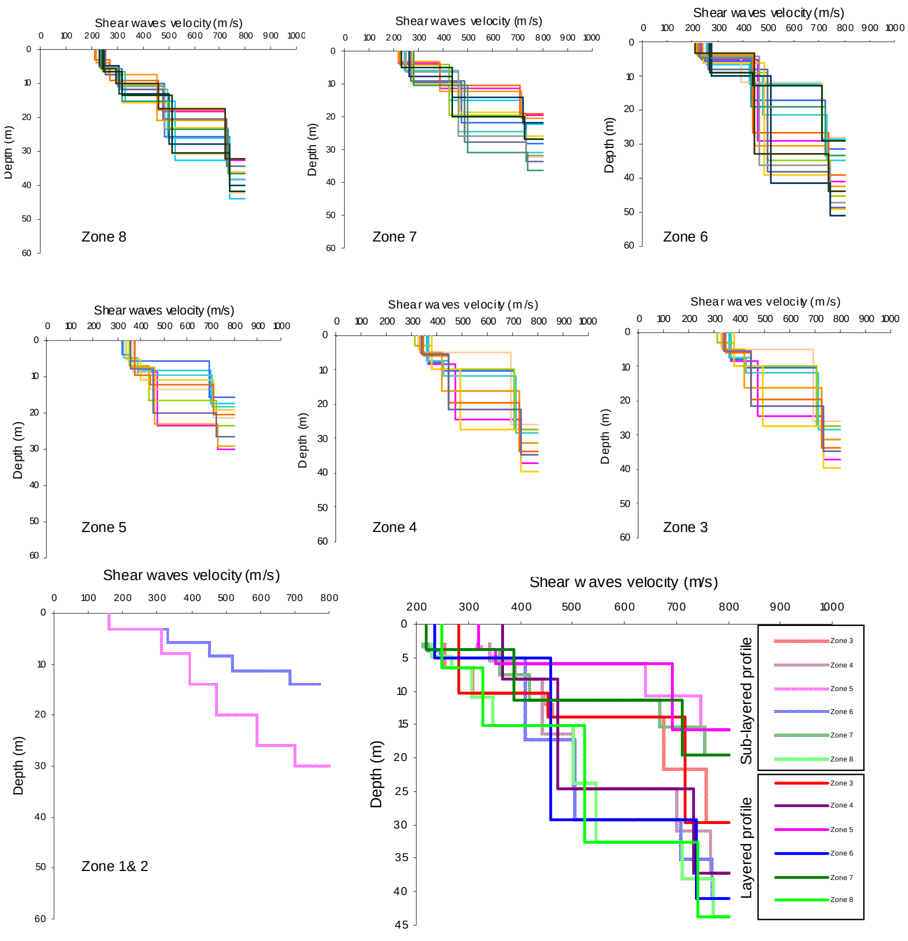

Fig. 7. Simulate layered Vs-profiles generated using the Monte Carlo technique. An example of some sub-layer divisions used in NERA analysis.

NHESSD
2, 963–997, 2014

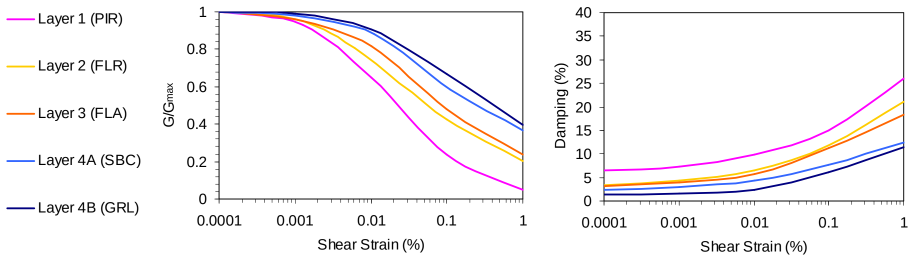

Fig. 8. Strain-dependent curves of shear normalized modulus, G/G_0, and damping curves, D/D_0 extracted from: Guadagno et al. (1998) for PIR; Zhang et al. (2005) for FLR, FLA SBC and GRL.

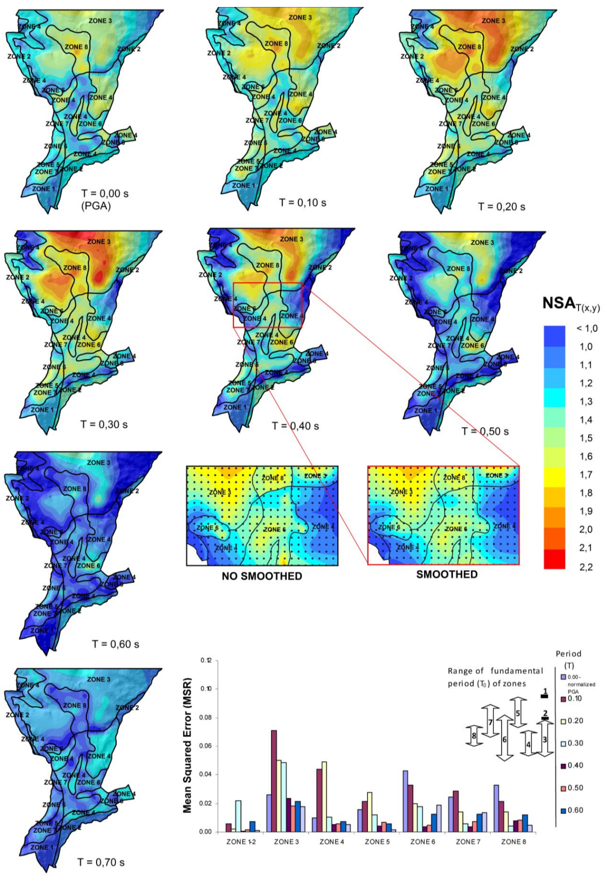

Fig. 9. Maps of normalized acceleration response spectra, NSA$_T$, with 5 % damping; an example of spatial smoothing using an under sampled regular mash of 50 m. In addition, the fitting errors in period-disaggregated analysis in terms of mean squared error are showed.

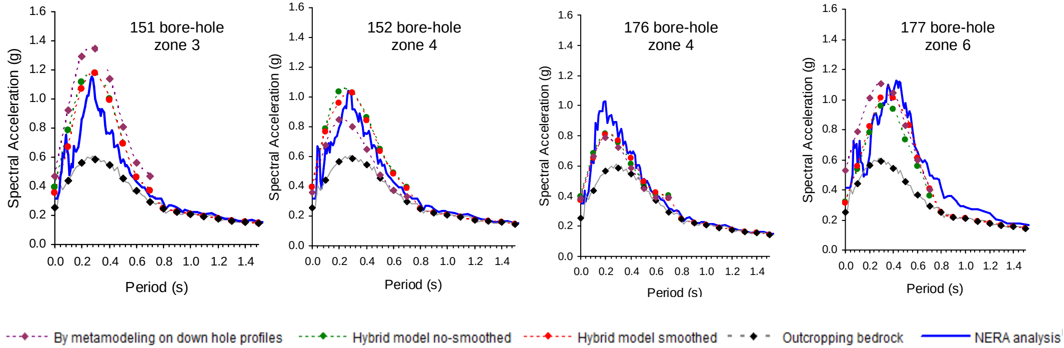

Fig. 10. Back-validation analysis performed in comparison to four experimental Vs-profiles.